Inorganic Chemistry

Article

pubs.acs.org/IC

Fine-Tuning the Luminescence and HOMO−LUMO Energy Levels in Tetranuclear Gold(I) Fluorinated Amidinate Complexes

Hanan E. Abdou,[†] Ahmed A. Mohamed,[§] José M. López-de-Luzuriaga,[‡] Miguel Monge,[‡] and John P. Fackler, Jr.*[,†]

[†]Department of Chemistry, Texas A&M University, College Station, Texas 77843, United States

[‡]Departamento de Química, Universidad de La Rioja, Grupo de Síntesis Química de La Rioja, UA-CSIC, Madre de Dios 51, E-26004 Logroño, Spain

[§]Department of Chemistry, Delaware State University, Dover, Delaware 19901, United States

Supporting Information

ABSTRACT: Tetranuclear gold(I) fluorinated amidinate complexes have been synthesized and their photophysical properties and structures described. DFT calculations were carried out to illustrate how a minor change in the ligand resulted in a loss of emission in the perfluorophenyl amidinate complex compared with nonfluorinated phenyl amidinate complexes reported previously. The fluorinated complexes reported here $[Au(ArN)_2C(H)]_4$ (**1**, Ar = 4-FC_6H_4; **2**, 3,5-$F_2C_6H_3$; **3**, 2,4,6-$F_3C_6H_2$; **4**, 2,3,5,6-F_4C_6H) emit in the blue-green region at 470, **1**, 478, **2**, 508, **3**, and 450 nm, **4**, by excitation at ca. 375 nm at room temperature with nanosecond lifetimes. The emissions observed at 77 K in the solid state show structured emission for complexes **1** and **2**, with a vibrational spacing of ca. 1200 and 1500 cm^{-1}, corresponding to the vibrational modes of the amidinate ligand. The pentafluorophenyl derivative **5**, Ar = C_6F_5, shows no photoluminescence in the solid state nor in the solution. This result is different from results in which the pentafluorophenyl group is attached to a phenylpyridine ligand in an Ir(III) complex and other organics. This quenching appears to be related to a nonradiative de-excitation process caused by the $\pi\pi^*-\pi\sigma^*$ crossover in the excited state of the pentafluorophenyl amidinate ligand. With increasing numbers of fluorine atoms, there is a progressive decrease in the contribution of the amidinate ligands to the corresponding HOMO orbital. There also is a slight decrease in the ligand contribution to the LUMO with increased numbers of fluorine atoms and an exchange of the character of the orbitals of the gold centers.

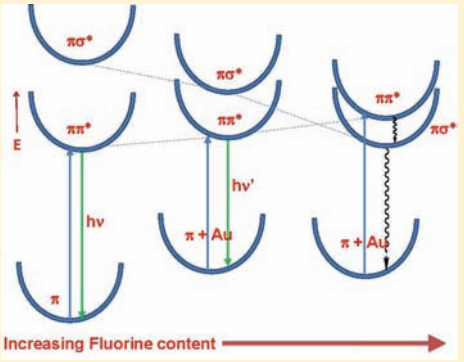

INTRODUCTION

The chemistry of group 11 nitrogen ligand complexes and gold in particular has witnessed a major expansion in synthesis and applications.[1] There are wide applications for these materials in medicine,[2] light emitting diodes fabrication,[3] catalysis,[4] chemical vapor deposition,[5] and liquid crystals.[6] This class of compounds is unique in the heterogeneous catalysis of CO oxidation by gold since metal−nitrogen precursors provide an attractive route for the preparation of chloride-free gold catalysts. A Au/TiO_2 catalyst, synthesized from a tetranuclear gold amidinate complex, showed the best performance for room temperature CO oxidation by nanogold.[7] Metal amidinates have been found to be suitable precursors for the Atomic Layer Deposition of transition metals and metal oxides.[8] Even with the growing number of experimental and theoretical studies, the detailed structures of the excited states in complexes with amidinate nitrogen ligands remains poorly understood and warrants further photophysical study.[1c]

Previously, several tetranuclear gold(I) amidinate complexes, $[Au(ArN)_2C(H)]_4$: Ar = $-C_6F_5$; 3-CF_3−Ph; 3,5-Cl_2−Ph; 4-OMe−Ph; 4-Me−Ph; 1-naphthyl], have been synthesized in our laboratory by the reaction of Au(THT)Cl with the potassium or sodium salt of the amidinate ligand in THF.[9a] Tetranuclear gold(I) amidinate complexes with groups on the NCN carbon, NC(Me)N and NC(Ph)N, were also prepared.[9b] Preliminary studies of the tetranuclear gold(I) amidinate complexes show luminescence differences with changes in the substituents on the phenyl rings. These differences likely are caused by the influence of each substituent on the electron rich, delocalized NCN linkage. The tetranuclear complexes $[Au(ArN)_2C(H)]_4$, Ar = 4-$OMeC_6H_4$, 3-$CF_3C_6H_4$, 4-MeC_6H_4, and 3,5-$Cl_2C_6H_3$, show bright blue-green fluorescence at room temperature. The tetranuclear 1-naphthyl derivative $[Au(C_{10}H_7N)_2C(H)]_4$ is luminescent only at 77 K. Surprisingly, the pentafluorophenyl derivative Ar = C_6F_5 did not show any observable photoluminescence in the solid state nor in the solution even at low temperatures. This contrasts with the data for the luminescence of an Ir(III) complex in which a pentafluorophenyl moiety is attached at different positions on

Received: May 19, 2011
Published: January 30, 2012

   dx.doi.org/10.1021/ic2010634 | *Inorg. Chem.* 2012, 51, 2010−2015

a phenylpyridine ligand.[1d,e] Furthermore, the pentafluorophenyl amidinate derivative $[Au(C_6F_5N)_2C(H)]_4$ did not show any oxidation below 1.8 V, in contrast to the other tetranuclear complexes with substituents such as Ar = 4-$OMeC_6H_4$, 4-MeC_6H_4, and 3,5-$Cl_2C_6H_3$, which showed three reversible waves.[9] We report here our study of the syntheses and spectroscopy of phenylamidinate gold(I) complexes of fluorinated amidinates with 1−5 fluorine atoms on the phenyl rings.

2. EXPERIMENTAL SECTION

2.1. Materials and Methods. All chemicals and reagents of reagent grade were commercially available and used without further purification. X-ray crystallographic data were collected as reported previously.[9]

2.2. Preparation of the Complexes. All the amidine ligands were synthesized according to modified literature procedure.[9] In these preparations, the aniline derivative, triethylorthoformate (orthoester) and a catalytic amount of acetic acid (1 mL), were mixed and the reaction mixture was heated to 140−160 °C in a reflux vessel for 1−2 h. The reaction mixture was distilled at the same temperature to remove the ethanol. The product was cooled to room temperature to form an off-white solid. The solid was recrystallized from THF/hexanes to give a white solid in 70−80% yield. The tetranuclear gold(I) amidinate complexes, $[Au(ArN)_2C(H)]_4$, Ar = **1**, 4-FC_6H_4; **2**, 3,5-$F_2C_6H_3$; **3**, 2,4,6-$F_3C_6H_2$; **4**, 2,3,5,6-F_4C_6H], were synthesized using the synthetic procedure described below for **4**. The yields were close to 70% for each complex. Details for the synthesis of each of the ligands are in the Supporting Information.

2.2.1. Synthesis of $[Au_4(ArNC(H)NAr)_4]$, Ar = 2,3,5,6-C_6HF_4, 4. *N,N′*-di(2,3,5,6-tetrafluoro)phenylformamidine (226 mg, 0.67 mmol) was stirred with 37 mg (0.67 mmol) of KOH in 20 mL of 50/50% THF/ethanol mixture for 24 h. Au(THT)Cl (213 mg, 0.67 mmol) was added, and stirring continued for an additional 4−5 h. The solution was filtered, and the volume was decreased under reduced pressure and hexanes was added to form an off-white precipitate. The product was filtered and recrystallized from THF/hexanes to give the tetranuclear gold(I) complex in 70% yield.

Anal. Calcd. for $C_{52}H_{36}F_8N_8Au_4$, **1**: C, 36.44; H, 2.10. Found: C, 36.15; H, 1.89. ^{19}F NMR ($CDCl_3$, ppm): −123 (bm, F4). ^{1}H NMR ($CDCl_3$, ppm): 8.2 (s, 4H, CH amidinate), 6.8 (16H), 7.0 (16H). Yield 70%. UV−vis (CH_2Cl_2) λ_{max} (nm), ε (L/M^{-1}cm^{-1}): 255-(26,490), 295(16,584), 325(12,012), 354(8,492), and 397(4,528).

Anal. Calcd. for $C_{52}H_{28}F_{16}N_8Au_4$, **2**: C, 33.64; H, 1.61. Found: C, 33.90; H, 1.75. ^{19}F NMR ($CDCl_3$, ppm): −112 (bm, F3,5). ^{1}H NMR ($CDCl_3$, ppm): 8.3 (s, 4H, CH amidinate), 6.5 (16H), 6.7 (8H). Yield 67.4%. UV−vis (CH_2Cl_2) λ_{max} (nm), ε (L/M^{-1}cm^{-1}): 255(18,646), 290(11,652), 318(10,732), and 353(4,974).

Anal. Calcd. for $C_{52}H_{20}F_{24}N_8Au_4$, **3**: C, 31.20; H, 1.00. Found: C, 31.40; H, 0.80. ^{19}F NMR ($CDCl_3$, ppm): −121 (bt, F4); −129 (bd, F2,6). ^{1}H NMR ($CDCl_3$, ppm): 7.9 (s, 4H, CH amidinate), 6.98(16H). Yield 75%. UV−vis (CH_2Cl_2) λ_{max} (nm), ε (L/M^{-1}cm^{-1}): 253(73,456), 275(46,236), 297(31,352), and 355(3,644).

Anal. Calcd. for $C_{52}H_{12}F_{32}N_8Au_4$, **4**: C, 29.10; H, 0.55. Found: C, 29.47; H, 0.50. ^{19}F NMR ($CDCl_3$, ppm): −143 (m, F3,5); −152 (b, F2,6). ^{1}H NMR ($CDCl_3$, ppm): 8.0 (s, 4H, CH amidinate); 6.9(8H). Yield 70%. UV−vis (CH_2Cl_2) λ_{max} (nm), ε (L/M^{-1}cm^{-1}): 258 (79,225), 272 (68,865), 293 (47,175), and 375 (2,090).

Anal. Calcd. for $C_{52}H_4F_{40}N_8Au_4$, **5**: C, 27.27; N, 4.89. Found: C, 27.75; N, 4.64. ^{19}F NMR ($CDCl_3$, ppm): −166 (bt, F4); −162 (t, F3,5); −153 (bd, F2,6). ^{1}H NMR ($CDCl_3$, ppm): 8.3 (s, 4H, CH amidinate). Yield 77%. UV−vis (CH_2Cl_2) λ_{max} (nm), ε (L/M^{-1}cm^{-1}): 260(102,800), 285(76,900), 300(46,700).

2.3. Computational Details. All calculations were performed using the Gaussian03 suite of programs.[10]

2.3.1. Hybrid DFT-B3LYP/UFF (QM/MM) ONIOM Calculations.[11] Hybrid quantum mechanical (DFT-B3LYP)[12]/molecular mechanical (Universal Force Field, UFF)[13] calculations were carried out for all atom model system. The quantum mechanical part was the tetranuclear metallic core and the amidinate ligand skeleton and was fully optimized at the DFT-B3LYP level. The molecular mechanics parts are the fluorinated rings on the N atoms, and they were treated with a Universal Force Field. The model systems were constrained to C_2 symmetry. The obtained optimized structures are very close to the experimental, although the gold···gold interaction distances are slightly larger than experimental ones (3.16−3.21 Å, theoretical, vs 2.93−2.97 Å, experimental). This trend is due to the fact that DFT methods are not able to reproduce completely the aurophilicity of the Au(I)···Au(I) interactions since all the correlation effects are not included at this level of calculation. Nevertheless, we have used this level of theory combined with the ONIOM methodology because these very large tetranuclear model systems can be optimized at an accessible computational cost.

2.3.2. DFT-B3LYP Single Point Calculations. Once the model systems were optimized using the ONIOM methodology, a single point energy calculation was performed for all model systems in order to analyze the electronic structures (HOMO and LUMO orbitals).

2.3.3. Basis Sets. The 19-valence electron (VE) quasirelativistic (QR) pseudopotential (PP) of Andrae[14] was employed for gold together with two f-type polarization functions (exponents, 0.2 and 1.19). The diffuse f-type function is required for describing the aurophilic attraction and the compact one for describing the covalent bonds.[15] The N, C, and F atoms were treated by Stuttgart pseudopotentials,[16] including only the valence electrons for each atom. For these atoms, double-ζ basis sets of ref 16 were used, augmented by d-type polarization functions.[17] For the H atom, a double-ζ plus a p-type polarization function were used.[18]

2.4. Crystallographic Studies. Cell parameters and refinement results from the check cif for the gold amidinate complex **4** are in an endnote[19] with the important distances listed in Table 2. X-ray data were collected using a Siemens (Bruker) SMART CCD (charge coupled device) based diffractometer equipped with a LT-2 low temperature apparatus operating at 110 K. A suitable crystal was chosen and mounted on a glass fiber using cryogenic grease. Data were measured using omega scans of 0.3° per frame for 60 s. The first 50 frames were recollected at the end of data collection as a monitor for decay. Unfortunately, the structure of **5** was not deemed suitable for publication although the .cif is included with this Article in the Supporting Information. No decay was detected for either structure. Cell parameters were retrieved using SMART software and refined using SAINT on all observed reflections. Data reductions were performed using SAINT software. The structures were solved by direct methods using SHELXS-97 and refined by least-squares on F2, with SHELXL-97 incorporated in SHELXTL-PC V 5.03. The structures were determined in the space groups reported in Table 1 by analysis of systematic absences. Hydrogen atom positions were calculated by geometrical methods and refined as a riding model.[20]

3. RESULTS AND DISCUSSION

3.1. Structures. Tetranuclear gold(I) fluorinated amidinate complexes, $[Au(ArN)_2C(H)]_4$, (Ar = **1**, 4-FC_6H_4; **2**, 3,5-$F_2C_6H_3$; **3**, 2,4,6-$F_3C_6H_2$; **4**, 2,3,5,6-F_4C_6H) are synthesized in 70−80% yield by the reaction between Au(THT)Cl and the potassium salt of the ligands in THF/ethanol, and the product was recrystallized from hexanes. Two tetranuclear structures $[Au(ArN)_2C(H)]_4$, Ar = 2,3,5,6-F_4C_6H, **4**, and C_6F_5, **5**, were characterized by X-ray crystallography, Figure 1 (see Supporting Information).

In both structures, each gold atom is coordinated to two amidinate ligands in a nearly linear coordination. The average Au···Au bond lengths in complexes **4** and **5** are ∼2.9 Å. The packing diagram of **4** and **5** shows weak Au···F (∼3.1 Å, intramolecular) and Au···F (∼3.55 Å, intermolecular) interactions.

3.2. Spectroscopic Results. The absorption data for complexes **1**−**4** are summarized in Table 1. The absorption

dx.doi.org/10.1021/ic2010634 | Inorg. Chem. 2012, 51, 2010−2015

Table 1. Spectroscopic and Photophysical Properties of Complexes 1−4

complex	medium/ (deg)	λ_{abs} [nm] (ε [mol^{-1}dm^{3}cm^{-1}])	λ_{em} (λ_{exc}) [nm]/τ (ns)
1	CH_2Cl_2 (298)	255 (26490), 295 (16584), 325 (12012), 354 (8492), 397 (4528)	
	solid (298)		470 (375) /102, 737
	solid (77)		462, 491, 532 (375)
2	CH_2Cl_2 (298)	255 (18646), 290 (11652), 318 (10732), 353 (4974)	
	solid (298)		478 (375) /169, 914
	solid (77)		505 (375)
3	CH_2Cl_2 (298)	253 (73456), 275 (46236), 297 (31352), 355 (3644)	
	solid (298)		508 (375) /142, 857
	solid (77)		490 (375)
4	CH_2Cl_2 (298)	258 (79225), 272 (68865), 293 (47175), 375 (2090)	
	solid (298)		450 (375) /59, 234
	solid (77)		447 (375)

spectra in 5 × 10^{-5} M CH_2Cl_2 at 298 K show in all cases intense peaks between 225 and 400 nm (Figure 2). The free ligands show the corresponding absorptions at 240−400 nm, and the potassium salts of these ligands show no observable luminescence. The resemblance of the absorption spectra for the amidinate complexes with those of the free amidine ligands suggests that the absorptions arise from ligand centered $\pi\rightarrow\pi^*$ transitions.

The four gold amidinate complexes, **1**−**4**, display a weak luminescence at room temperature and at 77 K in the solid state or in EtOH/MeOH/CH_2Cl_2 (8:2:1) glass media at 77 K, Table 1. Complexes $[Au(ArN)_2C(H)]_4$ (Ar = C_6H_4F **1**, $C_6H_3F_2$ **2**, $C_6H_2F_3$ **3**, and C_6HF_4 **4**) emit in the blue-green region at 470 **1**, 478 **2**, 508 **3**, and 450 nm **4** by excitation at ca. 375 nm at room temperature. The emissions observed at 77 K in the solid state are structured for complexes **1** and **2**, showing a vibrational spacing of ca. 1200 and 1500 cm^{-1}, Figure 2, corresponding to the vibrational modes of the amidinate ligand.[21] Complexes **3** and **4** do not display this vibronic

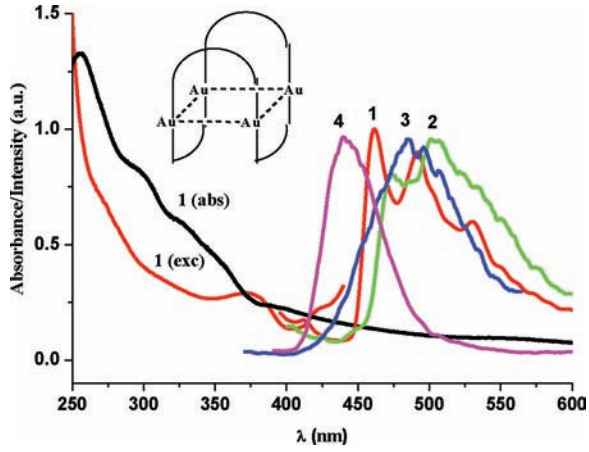

Figure 2. Absorption spectrum of **1** solution in 5 × 10^{-5} M CH_2Cl_2 (black), excitation (red), and emission spectra (red) in the solid state at 77 K. Emission spectra for **2** (green), **3** (blue), and **4** (magenta) in solid state at 77 K.

character, indicating a substantial difference in the excited state. The energies of the bands in the excitation spectra in the four complexes resemble the absorption spectra. This fact, together with the small separation between excitation and emission maxima and the lifetimes in the nanosecond range (**1**, 102.7 and 737.4; **2**, 169.4 and 914.5; **3**, 141.9 and 856.6; **4**, 59.1 and 433.8 ns) suggest that the transitions that are responsible for the emissions probably are heavy atom influenced fluorescence arising from the strong spin−orbit coupling of the four gold atoms. Also, the small shifts in the emissions from room temperature to liquid nitrogen temperatures imply that little structural change occurs from the ground state to the excited state consistent with ligand centered or LMCT (especially with **3** and **4**) transitions having little reorganizational behavior.

The weak absorption band at 397 nm for **1** was of some concern. Its origin is uncertain and may be associated with a Au···Au interaction as suggested by a referee. However, using an excitation frequency at 397 nm or elsewhere in the 300−420 nm range produced no change in the emission spectrum.

3.3. DFT Calculations. We have carried out a full optimization of model systems $[Au(ArN)_2C(H)]_4$, Ar = 4-C_6H_4F, **1**, 3,5-$C_6H_3F_2$, **2**, 2,4,6-$C_6H_2F_3$, **3**, 2,3,5,6-C_6HF_4, **4**, and 2,3,4,5,6-C_6F_5, **5**, using the ONIOM (QM/MM) DFT-B3LYP/

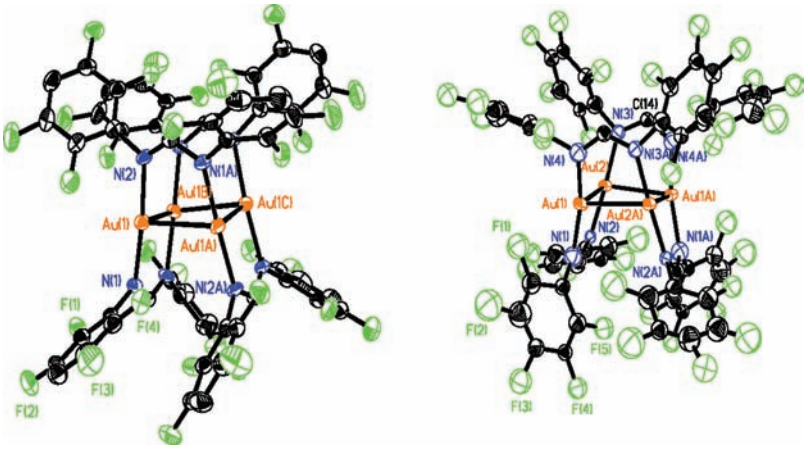

Figure 1. Thermal ellipsoid drawings of the tetranuclear gold(I) tetrafluorophenyl-, **4** (left), and pentafluorophenylamidinate, **5** (right), complexes at 50% probability.

dx.doi.org/10.1021/ic2010634 | *Inorg. Chem.* 2012, 51, 2010−2015

Table 2. Selected Theoretical (QM Part) and Experimental Structural Parameters for Model Systems 1−5 and Complexes 4 and 5[a]

	Au···Au	Au−N	N−C(H)	N−C_{ring}	N−Au−N	N−C−N
theor model **1**	3.163−3.165	2.045−2.048	1.323	1.417−1.418	176.71−176.73	124.73−124.75
theor model **2**	3.158−3.167	2.043−2.048	1.322	1.417−1.418	176.78−177.08	124.64−124.70
theor model **3**	3.215−3.216	2.042−2.048	1.322	1.418−1.419	173.55−173.81	124.89−124.93
theor model **4**	3.209−3.213	2.042−2.048	1.322	1.418−1.419	173.87−164.38	124.92−124.93
complex **4**	2.933−2.934	2.038−2.050	1.304−1.330	1.419−1.433	174.47−174.50	124.92−125.01
theor model **5**	3.213	2.043−2.048	1.322	1.418−1.419	173.95−174.23	124.96
complex **5**	2.954−2.971	1.967−2.087	1.311−1.339	1.397−1.485	167.96−171.68	124.60−126.13

[a]Distances are given in Å and angles in deg.

UFF level of theory. In order to save computational costs, we have calculated the perhalophenyl substituents using the Molecular Mechanics/UFF level, optimizing the rest of the molecule, i.e., the four gold atoms and the amidinate skeleton, at the DFT-B3LYP level of theory. The optimized structures are close to the experimental ones (see Table 2 for comparison) which makes these models valid for electronic structure analysis. The optimized Au−Au distances, although slightly larger, fall in the range of aurophilic interaction. It is important to note that the higher correlated method MP2 would lead to closer values, but the very large size of the model systems, between 1288 and 1640 basis functions for models **1** and **5**, respectively, would make these calculations very time-consuming.

The DFT calculations of the five models optimized at the ONIOM (QM/MM) DFT-B3LYP/UFF level of theory and based on the X-ray crystallographic data support the assignment of the emissive states. Thus, by looking at Figure 3, which

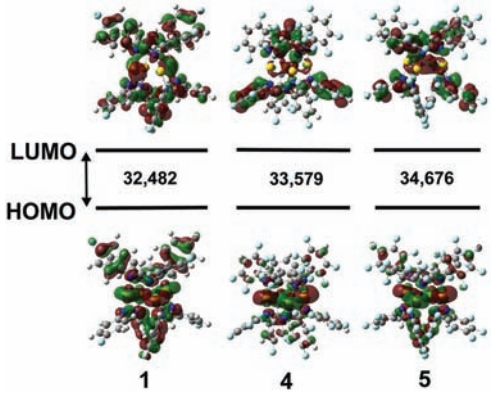

Figure 3. Frontier orbitals (HOMO and LUMO) for model systems $[Au(ArN)_2C(H)]_4$, (Ar = 4-FC_6H_4, **1**; 2,3,5,6-F_4C_6H, **4**; and C_6F_5, **5**). The HOMO−LUMO gaps are in cm^{-1} H atoms removed.

represents the orbital composition of the HOMO and LUMO orbitals for complexes **1**, **4**, and **5**, important differences in metal and ligand compositions can be noticed. A qualitative progressive decrease in the contribution of the amidinate ligands to the corresponding HOMO orbital is observed. When the fluorine content increases, there is a slight decrease in the ligand contributions and an exchange of the character of the orbitals of the gold centers in the LUMO (Supporting Information). The character of the orbitals of gold in the HOMO remains antibonding for the five models, while the LUMO is clearly antibonding for models **1** and **2** and bonding for model **5**. Additionally, the contribution of the gold centers to the LUMO orbitals in the models with more fluorine content is higher. A qualitative trend can be concluded by analyzing the composition of the frontier orbitals; the less fluorinated complexes **1** and **2** display a large π-ligand character both in the bonding HOMO and in the antibonding LUMO orbitals, leading to metal-perturbed intraligand transitions (IL), which relate to the vibrational structure observed in the emission spectra. When three **3** or four **4** fluorine atoms are placed on each phenyl ring, a Au $d_z^2\sigma^*$ character emerges in the HOMO, while the π^* character for the LUMO orbital is unchanged. This change, and the lack of vibronic character in the emissions of **3** and **4**, indicates a different vibronic coupling caused by the increased gold character in the corresponding wave functions.

In view of the electronic structures obtained from the DFT calculations and the experimental measurements for the five model gold fluoroamidinate systems, the photophysical properties appear theoretically predictable. The less fluorinated amidinate complexes **1** and **2** display structured emissions due to metal perturbed intraligand transitions with a low influence from the gold(I) centers, while the higher metal contribution to the frontier orbitals of the more fluorinated complexes **3** and **4** lead to highly metal-perturbed unstructured emissions, Figure 2. The fact that the pentafluorophenyl amidinate complex **5** is not luminescent appears to be related to a nonradiative de-excitation process caused by a $\pi\pi^*-\pi\sigma^*$ crossover in the pentafluorophenyl amidinate ligands.[22]

Fluorescence was not observed for the pentafluorophenyl amidinate complex, **5**. This contrasts with data obtained when a fluorinated phenyl ring is attached to various positions on a coordinated phenylpyridine ligand bonded to Ir(III).[1d,e] However, for the Ir(III) complex, both red and blue shifts were observed depending on the position of the attachment of the pentafluorophenyl ring. For **5**, DFT results show that the frontier orbital composition becomes mainly metal composed (ligand-perturbed). This change might have been expected to lead to a metal centered ^{3}(MC) excited state of the type Au $d_z^2\sigma^* \rightarrow$ Au $6s/6p\sigma$ and a long-lived phosphorescent emission; but this is not observed. The lack of a normal phosphorescent emission for this tetranuclear Au(I) complex is likely due to the $\pi\pi^*-\pi\sigma^*$ crossover in the pentafluorophenyl group attached to the coordinated amidinate, Figure 4. Zgierski, Lim, and co-workers studied the photophysics of fluorinated benzenes where this crossover was first observed.[22] The first excited states (S_1) of pentafluorobenzene and hexafluorobenzene (S_1 state of $\pi\sigma^*$ character) are different from that of the less fluorinated benzenes (S1 state of $\pi\pi^*$ character), and exhibit very small fluorescence yields and short fluorescence lifetimes.[22] Our results suggest that there is a strong coupling between the π states of the phenyl group and the amidinate π system. The electron withdrawing effect of the pentafluorinated

dx.doi.org/10.1021/ic2010634 | Inorg. Chem. 2012, 51, 2010−2015

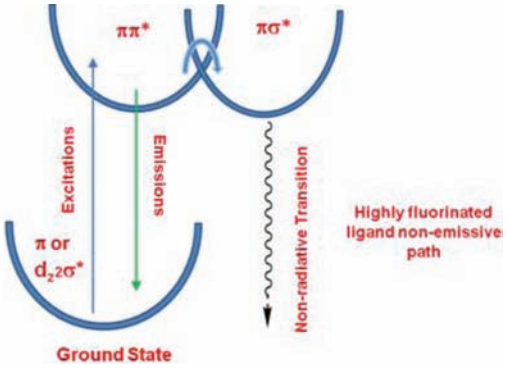

Figure 4. Schematic energy level diagram for the tetranuclear gold pentafluorophenylamidinate complex, **5**. The $\pi\pi^*-\pi\sigma^*$ crossover in the pentafluoroamidinate ligand appears to cause the luminescence to be quenched.[22]

phenyl ring also may be sufficient to prevent the observation of electrochemical oxidation waves for this complex in contrast to the reversible oxidation waves observed for the 3,5-dichlorophenyl and other less electron withdrawing amidinate ligand tetranuclear Au(I) complexes.

4. CONCLUSIONS

On the basis of the DFT calculations and the luminescence measurements for the gold fluoroamidinate complexes, the less fluorinated amidinate complexes display structured emissions due to metal-perturbed intraligand transitions with a low influence from the gold(I) centers, while the higher metal contribution to the frontier orbitals of the more fluorinated complexes lead to highly metal-perturbed unstructured LMCT emissions. The pentafluorinated amidinate complex, **5**, is not luminescent. This is consistent with a nonradiative de-excitation process caused by a $\pi\pi^*-\pi\sigma^*$ crossover in the perfluorophenyl amidinate ligands. Zgierski et al.[22] attributed this crossover to distortion of the benzene ring in the fluorinated benzenes. One suspects that there are other metal/ligand systems having a ligand excited state $\pi\pi^*-\pi\sigma^*$ crossover, which also show a similar LMCT emission quenching, although this apparently is not the case with the Ir(III) complexes having a pentafluorophenyl moiety attached to a phenylpyridine ligand.[1d,e]

■ ASSOCIATED CONTENT

Ⓢ Supporting Information

Syntheses of ligands and tetranuclear gold(I) amidinate complexes, computational details, CIF files of complexes **4** and **5**, ORTEPs of complexes **4** and **5**, frontier orbitals (HOMO and LUMO) for model systems **1**−**5**, and luminescence measurements. This material is available free of charge via the Internet at http://pubs.acs.org.

■ AUTHOR INFORMATION

Corresponding Author

*E-mail: fackler@chem.tamu.edu.

■ ACKNOWLEDGMENTS

The Robert A. Welch Foundation of Houston, Texas, is acknowledged for financial support to J.P.F. through grant No. A-0960. J.M.L-de-L. and M.M. thank the CTQ2010-20500-C02-02 for financial support.

■ REFERENCES

(1) (a) Abdou, H. E.; Mohamed, A. A.; Fackler, J. P., Jr. In *Gold Chemistry: Highlights and Future Directions*; Mohr, F., Ed.; Wiley & Sons: New York, 2009; Chapter 1, pp 1−45. (b) Mohamed, A. A. *Coord. Chem. Rev.* **2010**, *254*, 1918−1947. (c) Bojan, V. R.; Lopez-de-Luzuriaga, J. M.; Manso, E.; Monge, M.; Olmos, M. E. *Organometallics* **2011**, *30* (17), 4486−4489 and references therein. (d) Babudri, F.; Farinola, G. M.; Nasa, F.; Ragni, R. *Chem. Commun.* **2007**, 1003−1022. (e) Tsuzuki, T.; Shirasawa, T.; Suzuki, T.; Tokito, S. *Adv. Mater.* **2003**, *125*, 1455.

(2) For example, see (a) Corti, C.; Holliday, R. *Gold: Science and Applications*; CRC Press: Boca Raton, FL, 2010. (b) Messori, L.; Marcon, G. In *Metal Ions in Biological Systems*; Sigel, A., Sigel, H., Eds.; Marcel Dekker Inc.: New York, 2004; Vol. *42*.

(3) (a) Lo, S.-C.; Burn, P. L. *Chem. Rev.* **2007**, *107*, 1097. (b) Coe, B. J.; Curati, N. R. *Comments Inorg. Chem.* **2004**, *25*, 147.

(4) (a) Hashmi, A. S.; Toste, D. F., Eds. *Modern Gold Catalyzed Synthesis*; Wiley-VCH Verlag GmbH: New York, 2009. (b) Bond, G. C.; Louis, C.; Thompson, D. T. *Catalysis by Gold*, Catalytic Science Series; Imperial College Press: London, U.K., 2006; Vol. *6*.

(5) Kodas, T. T.; Hampden-Smith, M. J., Eds. *The Chemistry of Metal CVD*; Wiley-VCH: New York, 1994.

(6) Bardaji, M. In *Modern Supramolecular Gold Chemistry: Gold-Metal Interactions and Applications*; Laguna, A., Ed.; John Wiley & Sons: New York, 2008; p 403.

(7) (a) Yan, Z.; Chinta, S.; Mohamed, A. A.; Fackler, J. P. Jr.; Goodman, D. W. *J. Am. Chem. Soc.* **2005**, *127*, 1604. (b) Yan, Z.; Chinta, S.; Mohamed, A. A.; Fackler, J. P. Jr.; Goodman, D. W. *Catal. Lett.* **2006**, *111*, 15.

(8) Lim, B. S.; Rahtu, A.; Gordon, R. G. *Nat. Mater.* **2003**, *2*, 749.

(9) (a) Abdou, H. E.; Mohamed, A. A.; López-de-Luzuriaga, J. M.; Fackler, J. P. Jr. *J. Cluster Sci.* **2004**, *15*, 397. (b) Abdou, H. E.; Mohamed, A. A.; Fackler, J. P. Jr. *J. Cluster Sci.* **2007**, *18*, 630. (c) Abdou, H. A.; Mohamed, A.; López-de-Luzuriaga, J. M.; Fackler, J. P. Jr. *J. Chin. Chem. Soc.* **2007**, *54*, 1107−1113. The structure of **5** was not deemed to be of sufficient X-ray quality to be published, but the .cif file has been submitted with this Article.

(10) Frisch, M. J.; Trucks, G. W.; Schlegel, H. B.; Scuseria, G. E.; Robb, M. A.; Cheeseman, J. R.; Montgomery, J. A., Jr.; Vreven, T.; Kudin, K. N.; Burant, J. C.; Millam, J. M.; Iyengar, S. S.; Tomasi, J.; Barone, V.; Mennucci, B.; Cossi, M.; Scalmani, G.; Rega, N.; Petersson, G. A.; Nakatsuji, H.; Hada, M.; Ehara, M.; Toyota, K.; Fukuda, R.; Hasegawa, J.; Ishida, M.; Nakajima, T.; Honda, Y.; Kitao, O.; Nakai, H.; Klene, M.; Li, X.; Knox, J. E.; Hratchian, H. P.; Cross, J. B.; Bakken, V.; Adamo, C.; Jaramillo, J.; Gomperts, R.; Stratmann, R. E.; Yazyev, O.; Austin, A. J.; Cammi, R.; Pomelli, C.; Ochterski, J. W.; Ayala, P. Y.; Morokuma, K.; Voth, G. A.; Salvador, P.; Dannenberg, J. J.; Zakrzewski, V. G.; Dapprich, S.; Daniels, A. D.; Strain, M. C.; Farkas, O.; Malick, D. K.; Rabuck, A. D.; Raghavachari, K.; Foresman, J. B.; Ortiz, J. V.; Cui, Q.; Baboul, A. G.; Clifford, S.; Cioslowski, J.; Stefanov, B. B.; Liu, G.; Liashenko, A.; Piskorz, P.; Komaromi, I.; Martin, R. L.; Fox, D. J.; Keith, T.; Al-Laham, M. A.; Peng, C. Y.; Nanayakkara, A.; Challacombe, M.; Gill, P. M. W.; Johnson, B.; Chen, W.; Wong, M. W.; Gonzalez, C.; Pople, J. A. *Gaussian 03*, revision C.02; Gaussian, Inc.: Wallingford, CT, 2003.

(11) Vreven, T.; Morokuma, K. J. *Comput. Chem.* **2000**, *21*, 1419.

(12) (a) Becke, A. D. *J. Chem. Phys.* **1992**, *96*, 215. (b) Becke, A. D. *J. Chem. Phys.* **1993**, *98*, 5648. (c) Lee, C.; Yang, W.; Parr, R. G. *Phys. Rev. Lett.* **1998**, *B 37*, 785.

(13) Rappé, A. K.; Casewit, C. J.; Colwell, K. S.; Goddard, K. S. III; Skiff, W. M. *J. Am. Chem. Soc.* **1992**, *114*, 10024.

(14) Andrae, D.; Häusserman, U.; Dolg, M.; Stoll, H.; Preuss, H. *Theor. Chim. Acta* **1990**, *77*, 123.

(15) Pyykkö, P.; Runeberg, N.; Mendizabal, F. *Chem.—Eur. J.* **1997**, *3*, 1451.

(16) Bergner, A.; Dolg, M.; Küchle, W.; Stoll, H.; Preuss, H. *Mol. Phys.* **1993**, *80*, 1431.

(17) Huzinaga, S. *Gaussian Basis Sets for Molecular Calculations*; Elsevier: Amsterdam, 1984; p 16.

(18) Huzinaga, S. *J. Chem. Phys.* **1965**, *42*, 1293.
(19) Crystallographic parameters for **4**: $C_{52}H_{12}F_{32}N_8Au_4$; space group, *I*41/*a*; a = 21.85(3), b = 21.85(3), c = 11.41(3); $\alpha = \beta = \gamma$ = 90.00, V = 5445(17), Z = 4, fw = 2144.58; R (reflections) = 0.0361(2577) ; wR^2 (reflections) = 0.1187(3672). Crystal data for **5** recognizing that the data obtained is not publishable quality: $C_{52}H_4F_{40}N_8Au_4$; space group, *C*2/*c*; a = 30.64(3), b = 11.801(10), c = 21.78(2); $\alpha = \gamma$ = 90.00, β = 133.891(15), V = 5675.39; Z = 4; R (reflections) = 0.1281(1917) ; wR^2 (reflections) = 0.2132(4853).
(20) X-ray programs used are in ref 9a.
(21) Piraino, P.; Bruno, G.; Tresoldi, G.; Faraone, G.; Bomieri, G. *J. Chem. Soc., Dalton Trans.* **1983**, 2391−2395.
(22) (a) Zgierski, M. Z.; Fujiwara, T.; Lim, E. C. *Acc. Chem. Res.* **2010**, *43*, 506. (b) Zgierski, M. Z.; Fujiwara, T.; Lim, E. C. *J. Chem. Phys.* **2005**, *122*, 144312.

dx.doi.org/10.1021/ic2010634 | *Inorg. Chem.* 2012, 51, 2010−2015